Acta Geochim (2024) 43:97–109
https://doi.org/10.1007/s11631-023-00645-3

ORIGINAL ARTICLE

The co-transport of Cd(II) and nZnO in saturated soil packed column: effects of ionic strength and pH

Min Liao[1,2] · Guo Bin[1,2] · Yixin Luo[1,2] · Yuhao Zhang[1,2] · Kangyou Hu[1,2] · Xiongxiong Lu[1,2] · Xiaomei Xie[1,3]

Received: 22 May 2023 / Revised: 19 September 2023 / Accepted: 7 October 2023 / Published online: 25 October 2023

Abstract The rapid development and widespread use of ZnO nanoparticles (nZnO) in various industries have raised concerns about their potential environmental impact. Therefore, understanding the fate and role of nZnO in the natural environment is crucial for mitigating their hazardous effects on the environment and human safety. The purpose of the present study was to provide scientific support for understanding and eliminating the joint risk of nanoparticle and heavy metal pollution in the soil environment by revealing the co-transport characteristics of Cd(II) and ZnO nanoparticles (nZnO) in soil under different ionic strength (IS) and pH. The impacts of different IS and pH on the co-transport of Cd(II) and nZnO in a 20 cm long with an inner diameter of 2.5 cm acrylic column packed with 10 cm high soil samples were investigated in the present study. In the above system, a 500 μg L^{-1} Cd(II) loaded nZnO suspension pulse with varying IS or pH was introduced into the soil column for leaching over 5 PVs, followed up by 5 PVs background solutions without nZnO. The IS was 1, 10, or 50 mM NaCl, with pH6, or the pH was 6, 7 or 8 with 1 mM NaCl. Meanwhile, Sedimentation experiments for nZnO, adsorption of Cd(II) on soil, and nZnO, DLVO theory calculation for the same background condition were conducted. The presence of nZnO significantly increased the mobility of Cd(II) as a result of its strong adsorption capacity for nZnO-associated Cd(II). However, with the increase of IS, the co-transport of nZnO and Cd(II) was decreased and the retention of nZnO in the soil column due to more nZnO attended to aggregate and sediment during the transport and the decrease in the adsorption capacity of nZnO for Cd(II) by competition of Na^{+}. When pH was 6, 7, and 8, the co-transport of nZnO and Cd(II) increased with higher pH due to the lower electrostatic attraction between nZnO and soil under higher pH. Meanwhile, the DLVO theory was fitted to describe the above co-transport process of nZnO and Cd(II). More attention should be paid to the presence of nZnO on the migration of Cd(II) in the natural soil to control the potential risk of nanoparticles and heavy metals to the environment. The risk of co-transport of nZnO and Cd(II) might be controlled by adjusting IS and pH in the soil solution.

Keywords ZnO · Nanoparticles · Cadimium · Soil · Co-transport

✉ Xiaomei Xie
xiexiaomei@zju.edu.cn

Min Liao
liaomin@zju.edu.cn

[1] College of Environmental and Resource Science, Zhejiang University, Yuhangtang Road No.866, Hangzhou 310058, China

[2] Zhejiang Provincial Key Laboratory of Subtropical Soil and Plant Nutrition, Yuhangtang Road No.866, Hangzhou 310058, China

[3] National Demonstration Center for Experimental Environmental and Resources Education (Zhejiang University), Yuhangtang Road No.866, Hangzhou 310058, China

1 Introduction

As technology improves by leaps and bounds, the synthesis and utilization of nanoparticles have become an important step in the innovation of nanotechnology (Aqeel et al. 2022; Ying et al. 2022). For the past few years, the

superiority of optical properties and chemical reactivity of ZnO nanoparticles (nZnO) has rendered it the most popular metal oxide nanoparticles, and it has wide applications in various fields such as cosmetics (Dubey et al. 2022; Gómez-Llorente et al. 2022), catalytic materials (Roguai and Djelloul 2021; Zheng et al. 2022), textile industry (Patil et al. 2019; Shaban et al. 2016) and electronic components (Choi et al. 2020; Neupane et al. 2019; Shariatmadar and Pakdehi 2017). However, the rapid growth of the nanotechnology industry and the utilization of nZnO present a tough challenge for environmental protection. An increasing number of scientific evidence has shown the nZnO that end up in the soil and aquatic environment and their release and accumulation will pose a great threat to human health (de Campos et al. 2019; Du et al. 2018; Khan et al. 2021). Based on these reasons, figuring out the fate and transport process of nZnO in the natural environment is essential for controlling the hazardous effects on the environment and human safety.

Several researchers have explored the mechanism of different environmental conditions affecting the transport of nZnO in porous media. It has been reported that IS and ion types would significantly affect the transport of nZnO in saturated quartz sand and the deposition of nZnO increased with the augment of solution IS in both monovalent and divalent salt solution (Jiang et al. 2012). pH plays an important role in the dissolution of nZnO, and the dissolution of nZnO decreases sharply with the increase of pH. Under acidic conditions, more than 50% of Zn^{2+} is released into the solution; Under neutral pH conditions, ZnO is relatively stable and has low solubility. Under alkaline conditions, although nZnO will also be dissolved into Zn^{2+} ions because it will further form zinc hydroxide [$Zn(OH)_2$] and other precipitations, there are not many Zn^{2+} ions (Dong et al. 2016). As an important environmental factor, pH also has a great effect on the mobility of nZnO. It was observed that the transport of nZnO in silica sand-packed columns decreased as the pH of the solution increased from 3 to 11 (Kanel and Al-Abed 2011). As one of the most crucial terrestrial ecosystems, the soil is a key sink for anthropogenic and natural contamination and most of the pollutants would end up in the soil. However, few studies have researched the transport behavior of nZnO in soil-packed columns, and the migration characteristics of nZnO in soil may be different from those in other porous media.

Due to the large specific surface area of nZnO, it has a great adsorption capacity to act as a carrier for other contaminants to co-transport in the soil (Dhiman and Kondal 2021). Once the nanoparticles and other contaminants co-transport in the soil, the harm of nanoparticles and pollutants to the environment will be more serious. Cadmium (Cd) is widely used in industrial processes such as mining, metallurgy, batteries, pigments, and so on. Cd is considered one of the most important toxic elements in soil and can lead to chronic toxicity even at a low concentration level (Hu et al. 2020; Yang et al. 2018). Diseases such as itai-itai disease, renal failure, brain damage, pulmonary edema, and lung cancer have been shown in the case of human exposure to Cd toxicity (Pal and Maiti 2019). Therefore, it is crucial to comprehend the migration of Cd(II) in the soil, especially the co-transport characteristics with mobile nZnO which few studies have been done. It also needs to be noted that other metal ions contained in the soil may compete with nZnO and Cd (II) to adsorb to the surface of soil particles (Peng et al. 2015; French et al. 2009), and soil organic matter can also form complexes with metal ions or Cd(II), which makes both competitive adsorption and complexation reactions eventually affect the co-migration and bioavailability of nZnO and Cd(II) to a certain extent (Zhao et al. 2019; Fu et al. 2020).

This study aims to address the knowledge gaps regarding the co-transport behavior of nZnO and Cd(II) in soil-packed columns. Additionally, it investigates the mechanisms behind the effects of solution chemistry (IS and pH) on the co-transport characteristics. The findings from this study provide important references for the prevention and control of nanoparticle and heavy metal pollution in soil ecosystems.

2 Materials and methods

2.1 Soil and nZnO nanoparticles

Due to the thriving mining industry in Gansu Province, heavy metals have continuously accumulated in the soil and migrated vertically with rainfall and surface runoff, posing a significant threat to ecosystems and human health. Therefore, in this study, we collected surface soil (0–20 cm) from Longnan City, Gansu Province, and allowed it to naturally dry. Any debris, such as dry branches and fallen leaves, was removed, and the soil samples were ground through a 1 mm sieve for further analysis. The collected soil properties are shown in Table S1. Soil pH was determined by the glass calomel electrode methods (Zhang et al. 2022). $BaCl_2$-$MgSO_4$ forced exchange method was used to determine the cation-exchange capacity (CEC) of the soil sample (Zhang et al. 2022). The potassium dichromate external heating method was used to determine soil organic matter (Zhang et al. 2022). A Zetasizer instrument was used to determine soil Zeta potential (ξ-potential) (Zhang et al. 2022).

2.2 nZnO suspensions

The nZnO was purchased from Hangzhou Chentong Biochemical Technology Co., LTD. To prepare nZnO nanoparticle suspensions, 8 g nZnO was introduced into 2 L deionized water with pH 6, 7, 8 or with 1, 10, 50 mM NaCl by ultrasonic at room temperature for 30 min. After standing for 10 days, the suspensions passed through a 0.22 μm filter membrane to obtain the stock solution of the nZnO suspension. The purchased nZnO was scanned by X-Ray Diffraction Instrument (XRD) (Ultima IV, Rigaku Corporation, Japan) and scanning electron microscopy (SEM) (Regulus 8100, Hitachi Corporation, Japan). XRD and SEM analysis results of nZnO are shown in Figs. S1 and S2. It showed XRD pattern of prepared nZnO was consistent with the characteristic peak of the ZnO (JCPSD 99-0111) standard card. This suggests that the nZnO nanoparticles in the suspensions were pure.

2.3 Sedimentation experiments

The stability of nZnO against deposition in different background solutions was evaluated using sedimentation experiments, where changes in concentration were recorded. The relative concentration (C/C_0) of nZnO in the background solution was calculated, where C represented the nZnO concentration at a specific time, and C_0 represented the initial nZnO concentration.

2.4 The adsorption of Cd(II) on soil and nZnO

To conduct the adsorption of Cd(II) on soil, the soil was mixed with $Cd(NO_3)_2$ at varying concentrations (10–120 mg L^{-1}) in a 50 mL centrifuge tube. The mixtures were then vibrated at room temperature (25 ± 1 °C) for 24 h to achieve equilibrium. After a while, centrifuge the suspensions with 3000 rpm for 20 min. Then, to filter the suspensions through a 0.45 μm membrane.

Varying concentrations of $Cd(NO_3)_2$ solutions (10–120 mg L^{-1}) were added to nZnO suspensions, which were then vibrated for 24 h to allow the systems to reach equilibrium. After 20 min of centrifugation at 3000 rpm, the suspensions were filtered through a 0.45 μm membrane. To explore the impact of soil solution on the adsorption capacity of Cd(II) on nZnO 20 mL nZnO suspensions with different background conditions (The IS was 1, 10 or 50 mM NaCl with pH 6, or the pH was 6, 7 or 8 with 1 mM NaCl, pH was adjusted by 0.1 M H_2SO_4 or Na_2CO_3) and 10 mL soil solution (soil–water ratio 1:20, centrifuged at 3000 rpm for 20 min after 24 h of shaking) containing various concentration of $Cd(NO_3)_2$ were added to the 50 mL centrifuge tube. After equilibration, to centrifuge the suspensions with 3000 rpm for 20 min. Then, to filter the suspensions through a 0.45 μm membrane. LC-ICP-MS was used to determine Cd(II) concentration in the equilibrium solution.

Langmuir and Freundlich equations were used to describe the characteristics of isotherms adsorption of Cd(II) on soil and nZnO (Zhang et al. 2022).

2.5 Column transport experiments

The column transport experiments were performed in a 20 cm long with an inner diameter of 2.5 cm acrylic column which was packed with 10 cm high soil samples. The parameters of the column transport leaching simulation experiment are shown in Table S2. The soil column was first saturated with 10 PVs Deionized water (DIW) at a flow rate of 7.56 m d^{-1} using a peristaltic pump (Longer LEAD-2) prior to the co-transport experiments. This was followed by the introduction of the 10 PV desired background solution to pre-equilibrate the system. Then, nZnO suspensions in 1, 10, or 50 mM NaCl with pH 6, or the pH was 6, 7 or 8 with 1 mM NaCl background solution containing 500 μg L^{-1} Cd(II) was introduced into the soil column by pulse for 5 PVs immediately. At last, 5 PVs background solution was introduced into the soil column. Effluent samples were collected every 5 mL in the centrifuge tube, and the concentration of Cd(II) in the effluent samples was determined by LC-ICP-MS (PerkinElmer Nexlon 300X). The Cd(II) of inflow and outflow was divided into dissolved Cd(II) and nZnO-associated Cd. The supernatant solution obtained after centrifugation at 15,000 rpm for 30 min was considered as dissolved Cd(II), whereas the portion of inflow and outflow that was not subjected to centrifugation or filtration was regarded as total Cd(II). The discrepancy between total Cd(II) and dissolved Cd(II) was defined as nZnO-bound Cd(II). The results of DIW leached soil column containing 500 μg L^{-1} Cd(II) was used as the control group. In addition, the Centrifugal product (nZnO-associated Cd) was scanned by SEM.

2.6 Calculation of interaction forces between particles

The interaction force between soil and nZnO particles or nZnO and nZnO particle, which included Van der Waals (VDW) and electric double layer (EDL) force, was calculated by DLVO theory (Zhang et al. 2022).

3 Results and discussion

3.1 The sedimentation and aggregation of nZnO

3.1.1 The sedimentation and aggregation of nZnO in different IS

To better understand the characteristics of the nZnO, the sedimentation, and aggregation of nZnO in different IS were detected. The particle size of nZnO is an indicator to reflect the aggregation of nZnO, and the stability of nZnO can be acknowledged through sedimentation experiments. As shown in Table 1 and Fig. 1. With the increase of IS, nZnO shows an obvious agglomeration with the particle size increasing from 210.38 to 400.33 nm. At high IS, nZnO exhibited stronger sedimentation due to aggregation. After 9 h of standing, the C/C_0 of nZnO in different IS were 0.72 (1 mM), 0.64 (10 mM) and 0.57 (50 mM) respectively. The lower C/C_0 indicated higher nZnO instability. The effect of IS on sedimentation and aggregation is attributed to that Na^+ will surround the surface of nZnO, which influences the Coulomb force between nZnO particles and further leads to the aggregation and sedimentation of nZnO (Zhao et al. 2021).

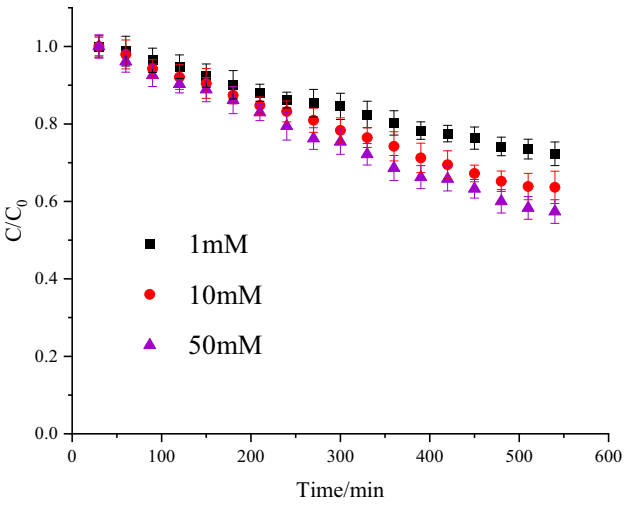

Fig. 1 Sedimentation kinetics of nZnO in different IS

3.1.2 The sedimentation and aggregation of nZnO in different pH

The sedimentation of nZnO increased slightly as the augmentation of pH value (Fig. 2). The C/C_0 of nZnO suspensions with pH of 6, 7, and 8 achieved 0.76, 0.75, and 0.72 respectively. The particle size of nZnO carrying positive charges increased from 290.34 to 361.84 nm as the value of pH increased from 6 to 8. The point of zero charges (pHpzc) location was approximately at pH 8.7–9.3 (Kanel and Al-Abed 2011; Mohd Omar et al. 2014), and when pH was closest to pHpzc, the electrostatic repulsion between nZnO was the smallest, which lead to obvious sedimentation of nZnO (Lu et al. 2015). The surface charge of nZnO decreased as the pH reached pHpzc, which resulted in the electrostatic repulsive force shrinking and agglomeration of nZnO. However, compared to the effect

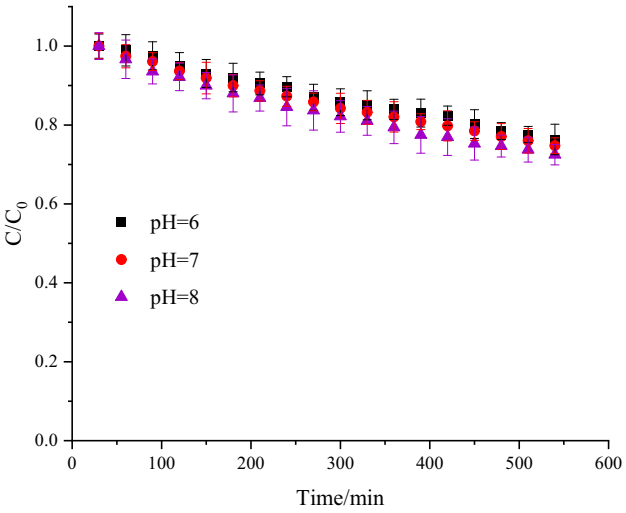

Fig. 2 Sedimentation kinetics of nZnO in different pH

Table 1 Partical size, Zeta potential and calculation of DLVO theory of nZnO in different background solution property

IS	pH	Particle size (nm)	Zeta potential (mV)	nZnO-nZnO		nZnO-soil	
				φ_{max} (K_BT)	φ_{min} (K_BT)	φ_{max} (K_BT)	φ_{min} (K_BT)
1	7	210.38 ± 12.47	− 12.83 ± 0.27	19.82	− 0.002	49.33	− 0.007
10	7	283.74 ± 18.48	− 9.74 ± 0.77	9.71	− 0.006	31.92	− 0.16
50	7	400.33 ± 12.45	− 7.53 ± 0.47	1.38	− 0.61	12.01	− 1.54
–	6	290.34 ± 24.33	8.78 ± 0.49	59.89	− 0.04	NA	NA
–	7	328.28 ± 19.28	5.86 ± 0.36	42.35	− 0.06	NA	NA
–	8	361.84 ± 30.54	3.17 ± 0.71	26.26	− 0.09	NA	NA

of IS on the sedimentation and aggregation of nZnO, the value of pH did affect the sedimentation and aggregation of nZnO but the impact was not as significant as IS in the range of pH 6–8.

3.2 Adsorption of Cd(II) on soil and nZnO

The purpose of the adsorption experiments is to investigate the possibility of simultaneous transport of nZnO and Cd(II). Meanwhile, the interaction of nZnO and Cd(II) can be explained through the adsorption experiments. In addition, soil solution is the basis of materials exchange between soil and the environment, as well as material migration and movement (Jiang et al. 2019). Therefore, investigations into the impact of soil solution on the adsorption of Cd(II) on nZnO were also carried out. The specific effects of different environmental factors on the adsorption are as follows.

3.2.1 The effect of IS on the adsorption

Fig. S3 displays the isothermal adsorption curves of Cd(II) under various ionic strengths. The Langmuir and Freundlich models were employed to fit the isothermal adsorption data. As depicted in Table 2, The isothermal adsorption curve of Cd(II) on soil can be well-fitted by both the Langmuir and Freundlich models. R^2 is the indicator to reflect the fitting degree of the models. In comparison, Langmuir models can better describe the adsorption of Cd(II) by soil and nZnO ($R^2 > 0.98$) which indicated that Cd(II) was adsorbed monolayer at uniformly distributed sites on the surface of the adsorbent (Azizian et al. 2018; Myachina et al. 2022). Table 2 shows that nZnO has a significantly higher maximum capacity to adsorb Cd(II) compared to soil. The nZnO has a larger specific surface area because of its nano features, thus its adsorption capacity is much stronger than that of soil. The maximum adsorption capacity of nZnO for Cd(II) also decreased significantly in the presence of soil solution. Such results might be attributed to competitive adsorption on the surface of nanoparticles by the coexisting metal ions or some soluble organic carbon (Kuang et al. 2020). But, nZnO could also overcome the competitive adsorption effect, and maintain a high Cd adsorption capacity, and could be a promising candidate for Cd(II) co-transport in soil systems.

The adsorption of Cd(II) on both soil and nZnO was significantly affected by the ionic strength (IS). The maximum adsorption capacities of Cd(II) in 1 to 10 mM and 50 mM NaCl background solution were 21.541, 14.741, 9.833 mg g^{-1} respectively. With the increase of IS, the maximum adsorption capacity of soil to Cd(II) gradually decreased. On the one hand, the presence of Na^+ ions led to competition for adsorption sites on the soil surface, resulting in a decrease in Cd(II) adsorption in soil (Li et al. 2022b; Wei et al. 2019). On the other hand, the IS affects the double electron layer structure of soil and thus affects its adsorption. However, the impact of IS on the adsorption of Cd(II) by soil is more noticeable in the adsorbate (Feizi et al. 2019). As a result, the primary factor that affects adsorption is ion competition, whereas the secondary factor is the alteration of the electric double-layer structure of soil (Gritti and Guiochon 2013; Hu et al. 2013; Tan et al. 2009).

The IS also has an obvious effect on the adsorption of nZnO to Cd(II). With the increase of IS, the maximum adsorption capacity of nZnO for Cd(II) shows a decreasing trend. High IS is not conducive to the adsorption of nZnO. At an IS of 50 mM, the maximum adsorption capacity of Cd(II) on nZnO was significantly lower at 152 mg g^{-1} compared to 205.631 mg g^{-1} at 1 mM. As the IS increased, Na^+ in the solution which can compete with the adsorption sites on the surface of nZnO with Cd(II) also increased. Therefore, the adsorption sites on the surface of

Table 2 Langmuir and Freundlich fitting results of Cd(II) adsorption isotherms by nZnO and soil in different IS

Materials	IS	Langmuir equation			Freundlich equation		
		Q_{max} (mg g^{-1})	K_L (m^3 g^{-1})	R^2	K_F (mg $g^{-1})^{1/n}$	n	R^2
Soil	1 mM	21.541 ± 0.114	0.159 ± 0.005	0.997	6.604 ± 1.676	0.358 ± 0.089	0.873
	10 mM	14.741 ± 0.649	0.024 ± 0.018	0.981	3.937 ± 1.117	0.359 ± 0.085	0.855
	50 mM	9.833 ± 0.598	0.035 ± 0.008	0.996	1.121 ± 0.314	0.496 ± 0.073	0.953
nZnO	1 mM	205.631 ± 17.396	0.015 ± 0.004	0.987	14.856 ± 3.087	0.556 ± 0.052	0.944
	10 mM	167.909 ± 9.075	0.010 ± 0.002	0.993	11.439 ± 2.614	0.568 ± 0.056	0.940
	50 mM	152.424 ± 8.880	0.006 ± 0.001	0.993	7.964 ± 1.989	0.616 ± 0.059	0.945
nZnO + soil solution	1 mM	104.331 ± 2.746	0.004 ± 0.001	0.989	13.256 ± 3.891	0.468 ± 0.071	0.861
	10 mM	83.754 ± 3.024	0.003 ± 0.001	0.980	9.498 ± 2.916	0.485 ± 0.074	0.863
	50 mM	69.682 ± 1.758	0.002 ± 0.001	0.987	7.068 ± 2.414	0.506 ± 0.079	0.862

nZnO tend to be saturated and the adsorption capacity is reduced (Li et al. 2022a). Under the condition of high IS, nZnO found an obvious agglomeration phenomenon, which means that it is more difficult for Cd(II) to contact the adsorption sites on the surface of nZnO. In addition, the increase of IS will compress the diffused electric double layer of nZnO (Dhiman and Sharma 2019; Pinheiro et al. 2020). On the one hand, Cd(II) is easier to contact with the adsorption sites, but on the other hand, it will destroy the bonding between the hydroxyl group and Cd(II) on the surface of nZnO (Jia et al. 2020).

3.2.2 The effect of pH on the adsorption

The isothermal adsorption curves at various pH values are presented in Fig. S4, and these curves were fitted using the Langmuir and Freundlich models. However, Langmuir is better fitted ($R^2 > 0.98$) for the adsorption of Cd(II) on nZnO which indicates that the adsorption of Cd(II) in the three systems with different pH is mainly monolayer adsorption (Chappell et al. 2022). The high adsorption capacity of nZnO in the presence of soil solution also indicated that nZnO has a high potential to facilitate the transport of Cd(II) in the soil at three pH values.

Table 3 indicates that the maximum adsorption capacity of soil for Cd(II) increased as the pH increased. Specifically, as the pH increased from 6 to 8, the maximum adsorption capacity of soil for Cd(II) increased from 16.176 to 27.187 mg g^{-1}. The impact of pH on the adsorption of Cd(II) is multifaceted. At first, H^+ can compete for the adsorption sites with Cd(II) in soil which leads to a decrease in the adsorption capacity of the soil (Zhao et al. 2014). With the increase in pH, the soil surface will be deprotonated, and the number of negative charges will increase, which is beneficial for the adsorption (Xu et al. 2022). Secondly, the increase in pH can enhance the stability of soil organic matter-metal complexes, thereby enhancing soil adsorption of Cd(II) (Fan et al. 2020; Yadav and Dasgupta 2022).

At pH 6, 7, and 8, nZnO exhibited maximum adsorption capacities for Cd(II) of 138.72, 182.155, and 197.945 mg g^{-1}, respectively. As the pH increased, the adsorption capacities of Cd(II) on nZnO showed a gradual increase trend as the pH increased (Fig. S4b). Despite the positive surface charge of nZnO at all three pH values, which is the same as that of Cd(II) in solution, nZnO still exhibited ideal adsorption capacities for Cd(II). The reason for this trend is that the higher pH can increase the number of hydroxyl groups on the surface of nZnO, which can bond more strongly with Cd(II) (Vargas et al. 2022). Additionally, the competition between H^+ and Cd(II) for adsorption sites and the tendency of nZnO particles to agglomerate are also significant factors affecting the adsorption of Cd(II) by nZnO (Godymchuk et al. 2020; Gupta et al. 2022).

3.3 Co-transport behavior of nZnO and Cd(II)

3.3.1 The effect of IS on the co-transport of nZnO and Cd(II)

As shown in Fig. S3, the strong adsorption capacity of nZnO indicated the potential for co-transport. Before conducting co-transport experiments, the amount of Cd(II) associated with nZnO and the amount of soluble Cd(II) in the influent were measured to determine if Cd(II) had been adsorbed onto the surface of nZnO. Therefore, it can be deduced that if the mobility of Cd(II) was promoted, it was in the form of nZnO-associated Cd(II). It can be seen from Fig. 3 that Cd(II) is difficult to penetrate the soil alone under three IS (14–16 μg L^{-1}). However, with nZnO assistance, the transshipment of Cd(II) was enhanced significantly, which was also observed by SEM (Fig. S5),

Table 3 Langmuir and Freundlich fitting results of Cd(II) adsorption isotherms by nZnO and soil in different pH

Materials	pH	Langmuir equation			Freundlich equation		
		Q_{max} (mg g^{-1})	K_L (m^3 g^{-1})	R^2	K_F (mg $g^{-1})^{1/n}$	n	R^2
Soil	6	16.176 ± 0.413	0.010 ± 0.003	0.944	1.633 ± 0.433	0.481 ± 0.063	0.875
	7	22.089 ± 1.027	0.008 ± 0.004	0.982	2.802 ± 0.957	0.489 ± 0.088	0.835
	8	27.187 ± 1.616	0.007 ± 0.005	0.962	2.901 ± 0.958	0.490 ± 0.089	0.838
nZnO	6	138.719 ± 9.069	0.001 ± 6.83E^{-4}	0.993	3.704 ± 1.312	0.716 ± 0.078	0.931
	7	182.150 ± 12.404	0.003 ± 0.001	0.994	5.809 ± 1.936	0.693 ± 0.075	0.911
	8	197.940 ± 12.328	0.005 ± 0.002	0.991	11.665 ± 3.668	0.592 ± 0.073	0.931
nZnO + soil solution	6	101.080 ± 4.264	0.002 ± 7.22E^{-4}	0.993	4.886 ± 1.717	0.634 ± 0.081	0.922
	7	126.108 ± 7.278	0.001 ± 8.24E^{-4}	0.983	6.978 ± 2.976	0.630 ± 0.101	0.887
	8	149.462 ± 7.890	0.014 ± 0.005	0.983	10.666 ± 2.615	0.564 ± 0.059	0.845

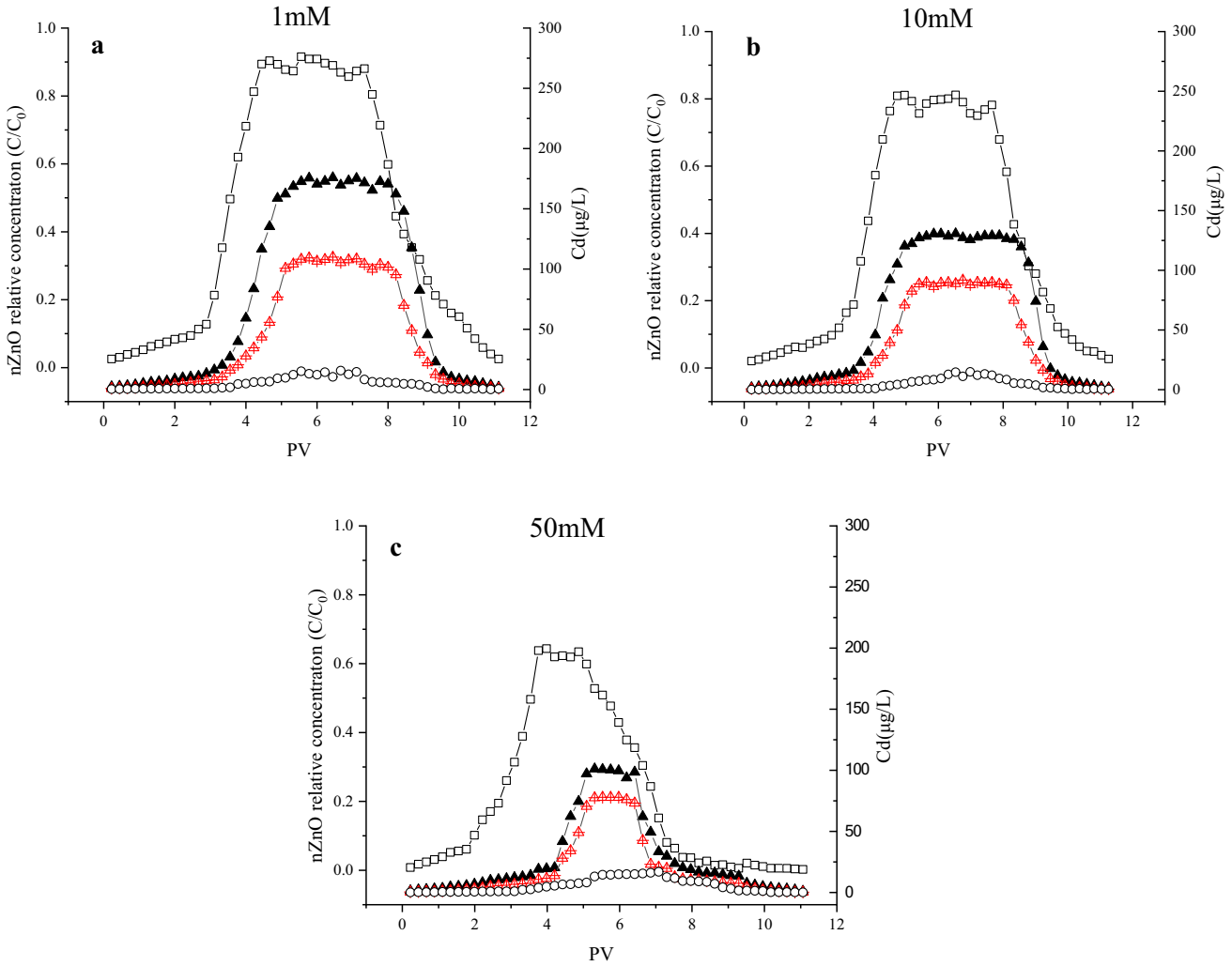

Fig. 3 The co-transport breakthrough curves of nZnO and Cd(II) in different IS (—▲— nZnO, —▲— total Cd(II) in the presence of nZnO, —△— soluble Cd(II) in the presence of nZnO, —○— total Cd(II) in the absence of nZnO)

most nZnO maintained a nanoparticle state, but its surface became smooth due to the adsorption of substances such as cadmium. The breakthrough curves of total Cd(II) were similar when the IS was 1 and 10 mM. After 4 PV the total concentration of Cd(II) in the effluent began to increase rapidly and reach a maximum value around 5 PV. After a plateau period of 4 PV, the total concentration of Cd(II) in the effluent decreased and became undetectable. On the other hand, for the case of nZnO, the relative concentration (C/C_0) of nZnO in the effluent increased after 3 pore volumes (PV) and reached its maximum C/C_0 at 4 PV. After a plateau period, the C/C_0 in the effluent sharply decreased at 8 PV. At 50 mM, the breakthrough curves of total Cd(II) and nZnO were significantly different, in which the total concentration of total Cd(II) in the effluent started to increase rapidly after 4 PV, reached a maximum around 5 PV, and then decreased after a short plateau. After 8 PV, little Cd(II) was found in effluent. However, the C/C_0 of nZnO in the effluent began to increase sharply after 2 PV, reached the maximum platform concentration at 3 PV, and decreased at around 5 PV. A long tail appeared in the descending stage and the relative C/C_0 of nZnO in breakthrough curves showed a trend of first increasing and then decreasing (ripening) (Jiang et al. 2012; Kretzschmar et al. 1999; Wang et al. 2015).

Table 2 demonstrates that the IS had a significant impact on the co-transport of nZnO. When the IS is 1, 10 and 50 mM, the maximum C/C_0 of Cd(II) in the effluent is 35.17% (175.86 μg L^{-1}), 26.13% (130.67 μg L^{-1}) and 20.23% (101.13 μg L^{-1}), and the portion of nZnO-associated Cd(II) are 47.54%, 25.07% and 15.40%, respectively. The maximum plateau relative concentration of nZnO decreases from 0.90 to 0.64 and more nZnO is retained in the soil. Under 50 mM NaCl, the plateau period of nZnO and Cd(II) is shortened which reflects that the transportability of Cd(II) changes with the change of nZnO.

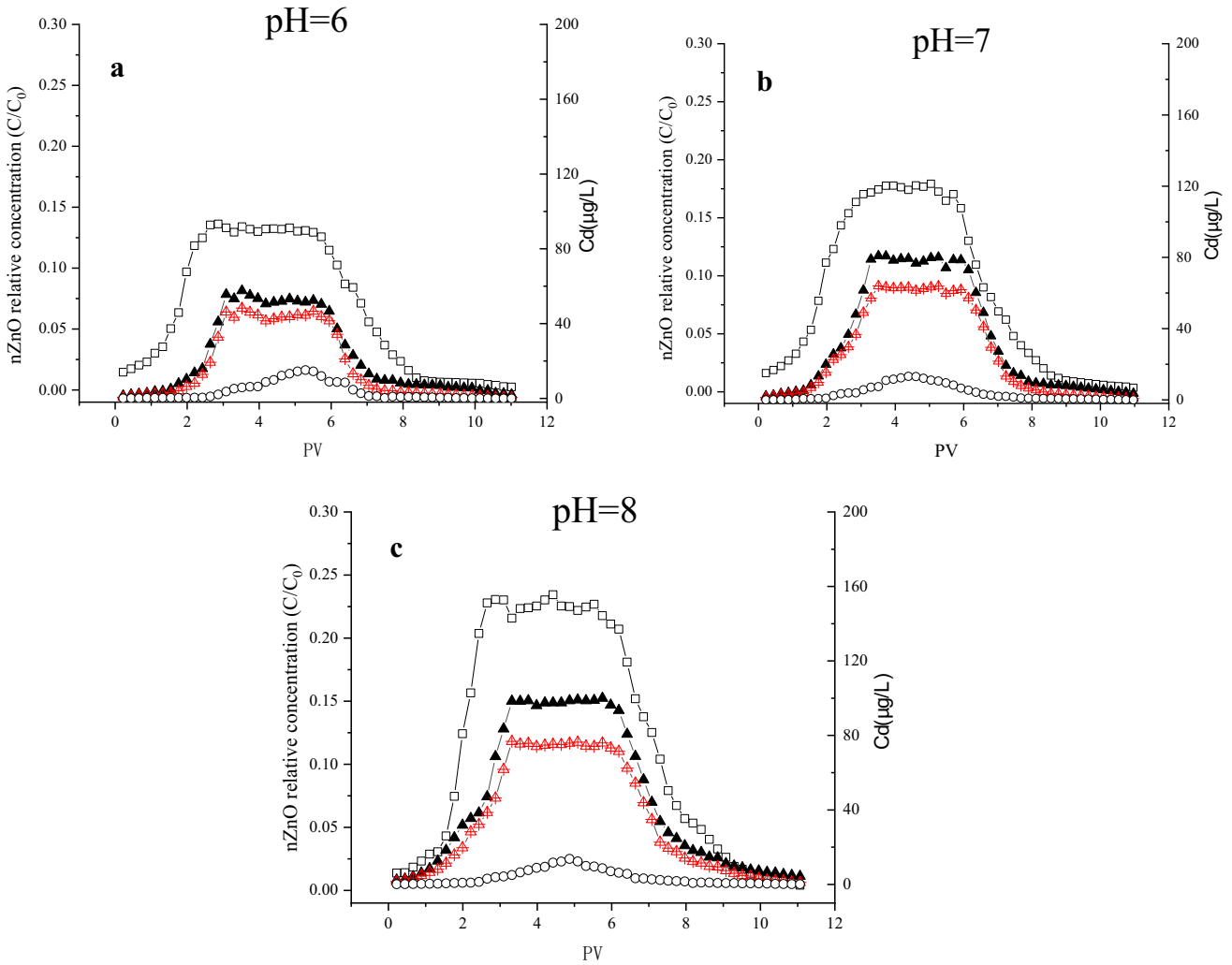

Fig. 4 The co-transport breakthrough curves of nZnO and Cd(II) in different pH (—□— nZnO, —▲— total Cd(II) in the presence of nZnO, —△— soluble Cd(II) in the presence of nZnO, —○— total Cd(II) in the absence of nZnO)

It further indicates that the co-transport of nZnO and Cd(II) is in the form of nZnO-association state. Combining the results of the adsorption experiments, it can be known that the adsorption capacities of nZnO to Cd(II) are the main reason for the decrease in co-transport (Fang et al. 2011). Meanwhile, the aggregation and sedimentation of nZnO lead to a decrease in its mobility in soil, which further weakens the co-transport of nZnO-associated Cd(II) (Fang et al. 2017; Zhou and Keller 2010). Additionally, because the soil is competitive for the adsorption of Cd(II) affected by Na^+, Cd(II) can be desorbed from the nZnO surface (Meng et al. 2022; Wang et al. 2022). In conclusion, the influencing factors of IS on co-transport included the adsorption capacities of nZnO for Cd(II), coagulation, and soil competitive adsorption.

3.3.2 The effect of pH on the co-transport of nZnO and Cd(II)

The breakthrough curves of the co-transport of nZnO and Cd(II) at different pH are shown in Fig. 4. The breakthrough curves under three pH conditions have a similar trend. The concentration of total Cd(II) in the effluent began to increase rapidly at 2 PV and reached the plateau around 3–4 PV. A sheer drop was observed at 6 PV, and little Cd(II) was detected after 9–10 PV. As for nZnO at three pH, the C/C_0 began to increase at about 2 PV, followed by the plateau of the relative concentration of nZnO. After 6 PV, it began to decrease and almost all nZnO had penetrated the soil column after 9 PV.

Table 4 Properties of the inflow and outflow

IS(mM)	pH	Influent		Effluent				
		nZnO-associated Cd(II) (%)[a]	Soluble Cd(II) (%)[b]	nZnO-associated Cd(II) (%)[c]	Soluble Cd(II) (%)[d]	Maximum C/C_0 of nZnO (%)	Maximum C/C_0 of Cd(II) (%)	Retention of nZnO (%)[e]
1	6	81.32	18.68	47.54	52.46	90.03	35.17	57.05
10	6	76.73	23.27	25.07	75.93	81.01	26.13	62.98
50	6	72.25	27.75	15.40	84.60	64.12	20.23	79.00
–	6	70.14	29.86	13.00	87.00	13.04	11.52	93.37
–	7	76.59	23.41	22.89	77.11	18.01	16.18	91.57
–	8	79.11	20.89	31.22	68.78	23.02	19.99	88.54

[a]Amount of Cd(II) adsorbed on nZnO compared to total Cd(II) in influent

[b]Amount of Cd(II) dissolved on nZnO compared to total Cd(II) in influent

[c]Amount of Cd(II) adsorbed on solution compared to total Cd(II) in effluent

[d]Amount of Cd(II) dissolved on nZnO compared to total Cd(II) in effluent

[e] Retention: $R = \frac{1}{n}\sum_{i=1}^{n}(1-\frac{C_i}{C_0})$ n: the sum of effluent; C_i: the concentration of nZnO in i-th effluent

Table 4 illustrates that pH had a significant impact on the transport of nZnO. With the increase in pH, the maximum C/C_0 of nZnO in effluent increased from 0.13 to 0.23. Moreover, the retention of nZnO decreased from 93.37% to 88.54% as the pH increased from 6 to 7 and the mobility of nZnO was significantly promoted. In the presence of nZnO, the maximum C/C_0 of total Cd(II) in the effluent for pH 6, 7, and 8 were 11.52% (57.6 μg L^{-1}), 16.18% (80.90 μg L^{-1}) and 19.99% (99.95 μg L^{-1}) respectively, while the portion of nZnO-associated Cd(II) were 13.00%, 22.89%, and 31.22% respectively. Besides adsorption, the influence of pH on the co-transport of nZnO and Cd(II) is also reflected in the surface charge of nZnO. At the three pH values, the Zeta potential of nZnO was positive, and the force between nZnO and soil was electrostatic attraction, which shows a high retention during the migration process (Xi et al. 2022). Nevertheless, the positive charge on the surface of nZnO decreased with the increase of pH, which resulted in a reduction of the electrostatic attraction between nZnO and soil. As a consequence, the co-migration ability increased (Mohd Omar et al. 2014). Although the aggregation and sedimentation of nZnO were more obvious at pH 8, the effects of aggregation and sedimentation on the co-transport were less than that of adsorption and electrostatic attraction caused by surface charge according to the column transport experiments.

3.3.3 DLVO interpretation of co-transport

It can be acknowledged from the results of DLVO theory that the maximum energy barrier (φ_{max}) of nZnO-nZnO decreases with the increase of IS (Fig. 5). The maximum energy barrier is just like a fence and only when the kinetic energy of nZnO particles after the collision is greater than the fence can they cross the energy barrier and thus aggregated and sediment (Delforce et al. 2021). As a result, the nZnO in 50 mM NaCl had a higher φ_{max} which indicated that the nZnO was easy to overcame the energy barrier and more nZnO tended to aggregate and sediment (Gomez-Flores et al. 2020). The interaction between nZnO and soil during co-transport can also be clarified through the DLVO theory. The φ_{max} of nZnO-soil decreased as the IS increased, and with an increase in IS, nZnO was more prone to surmount the barrier between nZnO and soil, leading to its deposition on the soil surface. In addition, The φ_{max} of nZnO-nZnO was lower than that of nZnO-soil and was more obvious under high IS which suggested that deposited nZnO on the soil surface can provide new adsorption sites for subsequent nZnO rather than being captured by the soil during the co-transport process(Samari Kermani et al. 2020). This was also the reason for the ripening observed in the co-transport at 50 mM.

4 Conclusion

This work intents to study the co-transport of nZnO and Cd(II) under the influence of IS and pH. It was found that the presence of nZnO significantly promoted the transport of Cd(II) in the form of nZnO-associated Cd(II) due to the great adsorption of nZnO on Cd(II). But the promotion of co-transport will be restrained with the increase of IS, which originates from the reduction in the adsorption capacity of nZnO for Cd(II) caused by Na^+ competing for adsorption sites on nZnO, as well as the increased

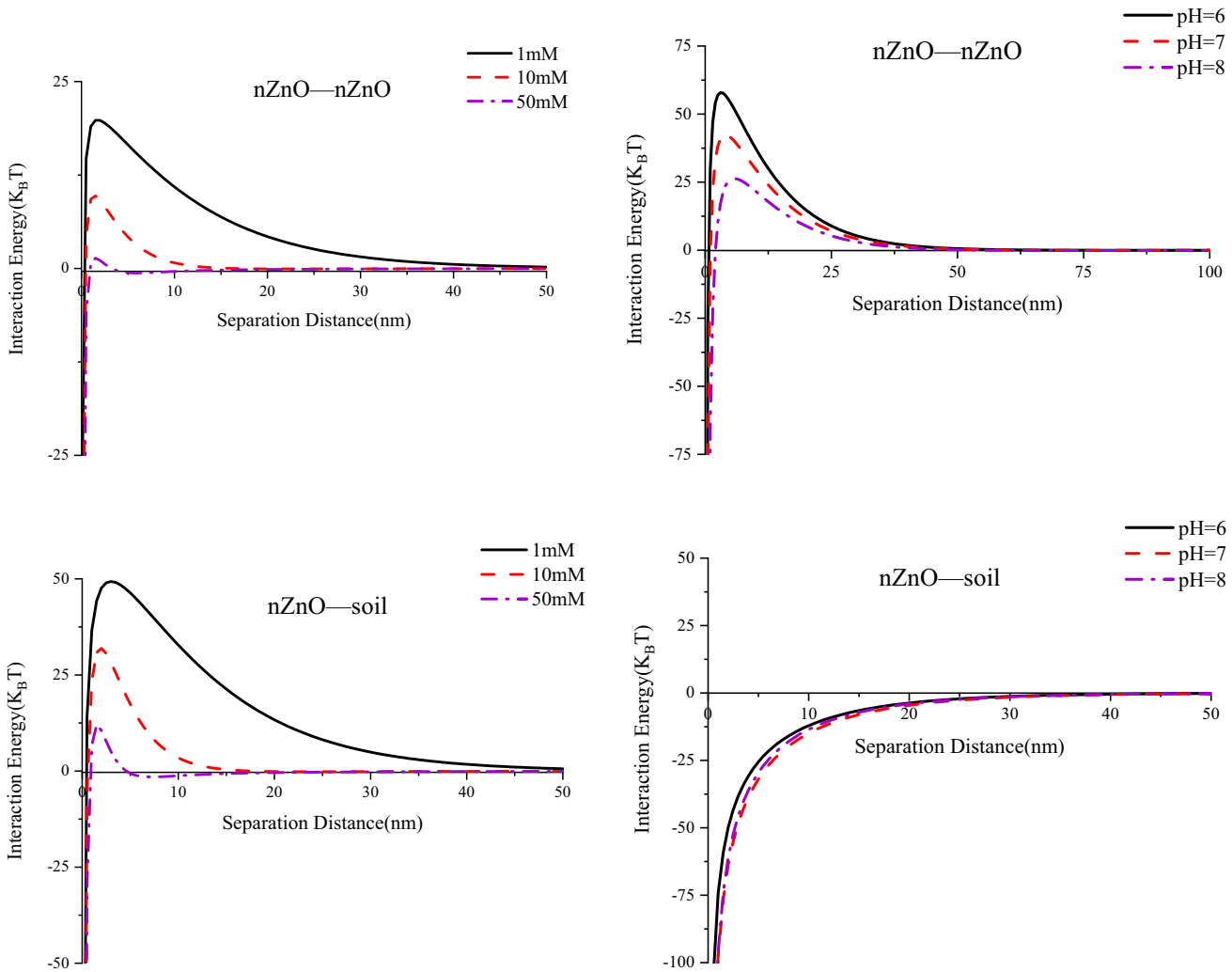

Fig. 5 DLVO interaction forces for nZnO-nZnO and nZnO-soil in different IS and pH

agglomeration and sedimentation of nZnO in the soil column due to high IS. The co-transport of nZnO and Cd(II) was also affected by pH. With the increase of pH, the particle size of nZnO gradually increases, the positive charge on the surface decreases, and the Zeta potential gradually decreases, and the maximum adsorption capacity of nZnO and Cd(II) shows a gradual increase trend. At the same time, the electrostatic attraction between nZnO and the soil decreases, resulting in an increase in co-migration capacity. When nZnO is relatively close to the pH zero electric point (PZC) at pH 8, the electrostatic repulsion between the nanoparticles is minimal and the adsorption capacity is also maximum, which may be due to the hydroxyl group on the surface of nZnO can bond with Cd(II) at higher pH. However, the effect of agglomeration and sedimentation on the co-transport was not significant in the pH range of 6–8. These characteristics of co-transport of nZnO and Cd(II) in soil column were supported well by the DLVO theory. In conclusion, the above observations suggest that more attention should be paid to the presence of nZnO in the migration of Cd(II) in the natural soil in order to control the potential risk of nanoparticles and heavy metals to the environment. Furthermore, it is important to note that the findings of this study are specific to the soil type investigated. Therefore, further research should be conducted when attempting to extrapolate these results to other soil types.

Supplementary Information The online version contains supplementary material available at https://doi.org/10.1007/s11631-023-00645-3.

Acknowledgements This work was supported by the National Key Research and Development Project of China and the National Natural Science Fund of China (Grant number 2018YFC1800403, 41571226).

Author contributions Min Liao and Xiaomei Xie conceived the idea. Min Liao and Xiaomei Xie designed the research. Bin Guo, Yuhao Zhang, Yixin Luo, Kangyou Hu, Xiongxiong Lu and Xiaomei Xie performed the experiment. Min Liao, Xiaomei Xie and Yuhao

Zhang analysed the data and wrote the manuscript. All authors contributed to the discussion of the manuscript.

Availability of data and materials All data generated or analysed during this study are included in this published article and its supplementary information files.

Declarations

Conflict of interest The authors declare that they have no known competing financial interests or personal relationships that could have appeared to influence the work reported in this paper.

Ethical approval This article dose not contain any studies with human or animal subjects performed by either of authors.

Consent to participate Not applicable.

Consent for publication All authors have read the submitted version of the manuscript and agree to submit the work to Environmental Science and Pollution Research, and we all agree that the transfer of copyright from the author to Environmental Science and Pollution Research.

References

Aqeel U, Aftab T, Khan MMA, Naeem M, Khan MN (2022) A comprehensive review of impacts of diverse nanoparticles on growth, development and physiological adjustments in plants under changing environment. Chemosphere 291:132672

Azizian S, Eris S, Wilson LD (2018) Re-evaluation of the century-old Langmuir isotherm for modeling adsorption phenomena in solution. Chem Phys 513:99–104

Chappell M, LeMonte J, McGrath C, Karna R, Styles R, Miller C, Miller L, Waites M, Middleton M, Price C, Chappell C, Dozier H, Abraham A, Henslee A, Strelzoff A (2022) Predicting Langmuir model parameters for tungsten adsorption in heterogeneous soils using compositional signatures. Geoderma 422:115924

Choi JH, Park T, Hur J, Cha HY (2020) AlGaN/GaN heterojunction hydrogen sensor using ZnO-nanoparticles/Pd dual catalyst layer. Sens Actuators B Chem 325:128946

De Campos RP, Chagas TQ, Da Silva Alvarez TG, Mesak C, De Andrade Vieira JE, Paixao CFC, De Lima Rodriguest AS, De Menezes IPP, Malafai G (2019) Analysis of ZnO nanoparticle-induced changes in Oreochromis niloticus behavior as toxicity endpoint. Sci Total Environ 682:561–571

Delforce L, Hofmann E, Nardello-Rataj V, Aubry JM (2021) TiO_2 nanoparticle dispersions in water and nonaqueous solvents studied by gravitational sedimentation analysis: complementarity of Hansen Parameters and DLVO interpretations. Colloids Surf A Physicochem Eng Asp 628:127333

Dhiman V, Kondal N (2021) ZnO Nanoadsorbents: a potent material for removal of heavy metal ions from wastewater. Colloids Interface Sci Commun 41:100380

Dhiman N, Sharma N (2019) Removal of pharmaceutical drugs from binary mixtures by use of ZnO nanoparticles. Environ Technol Innov 15:100392

Dong JZ, Liu ZF, Dong JF, Ariyanti D, Niu ZJ, Huang SF, Zhang WJ, Gao W (2016) Self-organized ZnO nanorods prepared by anodization of zinc in NaOH electrolyte. RSC Adv 6:72968–72974

Du LJ, Xiang K, Liu JH, Song ZM, Liu Y, Cao AN, Wang HF (2018) Intestinal injury alters tissue distribution and toxicity of ZnO nanoparticles in mice. Toxicol Lett 295:74–85

Dubey SK, Dey A, Singhvi G, Pandey MM, Singh V, Kesharwani P (2022) Emerging trends of nanotechnology in advanced cosmetics. Colloids Surf B 214:112440

Fan Y, Zheng C, Liu H, He C, Shen Z, Zhang TC (2020) Effect of pH on the adsorption of arsenic(V) and antimony(V) by the black soil in three systems: performance and mechanism. Ecotoxicol Environ Saf 191:110145

Fang J, Shan XQ, Wen B, Lin JM, Owens G, Zhou SR (2011) Transport of copper as affected by titania nanoparticles in soil columns. Environ Pollut 159:1248–1256

Fang J, Shijirbaatar A, Lin DH, Wang DJ, Shen B, Sun PD, Zhou ZQ (2017) Stability of co-existing ZnO and TiO_2 nanomaterials in natural water: aggregation and sedimentation mechanisms. Chemosphere 184:1125–1133

Feizi M, Jalali M, Antoniadis V, Shaheen SM, Ok YS, Rinklebe J (2019) Geo- and nano-materials affect the mono-metal and competitive sorption of Cd, Cu, Ni, and Zn in a sewage sludge-treated alkaline soil. J Hazard Mater 379:120567

French RA, Jacobson AR, Kim B, Baveye PC (2009) Influence of ionic strength, pH, and cation valence on aggregation kinetics of titanium dioxide nanoparticles. Environ Sci Technol 43:1354–1359

Fu YH, Wan Q, Qin ZH, Nie X, Yu WB, Li SS (2020) The effect of pH on the sorption of gold nanoparticles on illite. Acta Geochimica 02:172–180

Godymchuk A, Papina I, Karepina E, Kuznetsov D (2020) Behavior of ZnO nanoparticles in glycine solution: pH and size effect on aggregation and adsorption. Colloids Interface Sci Commun 39:100318

Gomez-Flores A, Bradford SA, Hwang G, Choi S, Tong M, Kim H (2020) Shape and orientation of bare silica particles influence their deposition under intermediate ionic strength: a study with QCM–D and DLVO theory. Colloids Surf A Physicochem Eng Asp 599:124921

Gómez-Llorente H, Hervás P, Pérez-Esteve É, Barat JM, Fernández-Segovia I (2022) Nanotechnology in the agri-food sector: consumer perceptions. NanoImpact 26:100399

Gritti F, Guiochon G (2013) Effect of the ionic strength on the adsorption process of an ionic surfactant onto a ^{18}C-bonded charged surface hybrid stationary phase at low pH. J Chromatogr A 1282:46–57

Gupta NK, Bae J, Baek S, Kim KS (2022) Sulfur dioxide gas adsorption over ZnO/Zn-based metal-organic framework nanocomposites. Colloids Surf A Physicochem Eng Asp 634:128034

Hu YQ, Guo T, Ye XS, Li Q, Guo M, Liu HN, Wu ZJ (2013) Dye adsorption by resins: effect of ionic strength on hydrophobic and electrostatic interactions. Chem Eng J 228:392–397

Hu BF, Shao S, Ni H, Fu ZY, Hu LS, Zhou Y, Min XX, She SF, Chen SC, Huang MX, Zhou LQ, Li Y, Shi Z (2020) Current status, spatial features, health risks, and potential driving factors of soil heavy metal pollution in China at province level. Environ Pollut 266:114961

Jia H, Wu HY, Wu T, Song JY, Dai JJ, Huang WJ, Huang P, Yan H, Lv KH (2020) Investigation on the adsorption mechanism and model of didodecyldimethylammonium bromide on ZnO nanoparticles at the oil/water interface. Colloids Surf A Physicochem Eng Asp 585:124159

Jiang XJ, Tong MP, Lu RQ, Kim HJ (2012) Transport and deposition of ZnO nanoparticles in saturated porous media. Colloids Surf A Physicochem Eng Asp 401:29–37

Jiang XQ, Zhang MY, Yan BG, Hu JW, Chen JY, Guan YT (2019) Roles of Mg-Al layered double hydroxides and solution chemistry on P transport in soil. Chem Eng J 373:1111–1119

Kanel SR, Al-Abed SR (2011) Influence of pH on the transport of nanoscale zinc oxide in saturated porous media. J Nanopart Res 13:4035–4047

Khan M, Khan MSA, Borah KK, Goswami Y, Hakeem KR, Chakrabartty I (2021) The potential exposure and hazards of metal-based nanoparticles on plants and environment, with special emphasis on ZnO NPs, TiO_2 NPs, and AgNPs: a review. Environ Adv 6:100128

Kretzschmar R, Borkovec M, Grolimund D, Elimelech M (1999) Mobile subsurface colloids and their role in contaminant transport. Adv Agron 66:121–193

Kuang XL, Shao JH, Peng L, Song HJ, Wei X, Luo S, Gu JD (2020) Nano-TiO_2 enhances the adsorption of Cd(II) on biological soil crusts under mildly acidic conditions. J Contam Hydrol 229:103583

Li D, Yang GJ, Chen MY, Pang L, Guo YB, Yu JH, Li T (2022a) Na co-cations promoted stability and activity of Pd/SSZ-13 for low-temperature NO adsorption. Appl Catal B 309:121266

Li H, Wang T, Su CX, Wu JF, Van der Meeren P (2022b) Effect of ionic strength on the sequential adsorption of whey proteins and low methoxy pectin on a hydrophobic surface: a QCM-D study. Food Hydrocoll 122:107074

Lu J, Liu DM, Yang XN, Liu HX, Liu SG, Tang H (2015) Sedimentation of TiO_2 nanoparticles in aqueous solutions: influence of pH, ionic strength, and adsorption of humic acid. Desalination Water Treat 57:18817–18824

Meng Z, Xu T, Huang S, Ge H, Mu W, Lin Z (2022) Effects of competitive adsorption with Ni(II) and Cu(II) on the adsorption of Cd(II) by modified biochar co-aged with acidic soil. Chemosphere 293:133621

Mohd Omar F, Abdul Aziz H, Stoll S (2014) Aggregation and disaggregation of ZnO nanoparticles: influence of pH and adsorption of Suwannee River humic acid. Sci Total Environ 468–469:195–201

Myachina M, Gavrilova N, Nazarov V (2022) Adsorption of molybdenum blue nanoparticles on the alumina surface. Colloids Surf A Physicochem Eng Asp 644:128819

Neupane GP, Ma WD, Yildirim T, Tang YL, Zhang LL, Lu YR (2019) 2D organic semiconductors, the future of green nanotechnology. Nano Mater Sci 1:246–259

Pal D, Maiti SK (2019) Abatement of cadmium (Cd) contamination in sediment using tea waste biochar through meso-microcosm study. J Clean Prod 212:986–996

Patil GD, Patil AH, Jadhav SA, Patil CR, Patil PS (2019) A new method to prepare superhydrophobic cotton fabrics by post-coating surface modification of ZnO nanoparticles. Mater Lett 255:126562

Peng YH, Tso CP, Tsai YC, Zhuang CM, Shihe YH (2015) The effect of electrolytes on the aggregation kinetics of three different ZnO nanoparticles in water. Sci Total Environ 530:183–190

Pinheiro D, Sunaja Devi KR, Jose A, Rajiv Bharadwaj N, Thomas KJ (2020) Effect of surface charge and other critical parameters on the adsorption of dyes on SLS coated ZnO nanoparticles and optimization using response surface methodology. J Environ Chem Eng 8:103987

Roguai S, Djelloul A (2021) Structural, microstructural and photocatalytic degradation of methylene blue of zinc oxide and Fe-doped ZnO nanoparticles prepared by simple coprecipitation method. Solid State Commun 334–335:114362

Samari Kermani M, Jafari S, Rahnama M, Raoof A (2020) Direct pore scale numerical simulation of colloid transport and retention. Part I: Fluid flow velocity, colloid size, and pore structure effects. Adv Water Resour 144:103694

Shaban M, Abdallah S, Khalek AA (2016) Characterization and photocatalytic properties of cotton fibers modified with ZnO nanoparticles using sol–gel spin coating technique. Beni-Suef Univ J Basic Appl Sci 5:277–283

Shariatmadar FS, Pakdehi SG (2017) Synthesis and characterization of aviation turbine kerosene nanofuel containing boron nanoparticles. Appl Therm Eng 112:1195–1204

Tan XL, Fang M, Li JX, Lu Y, Wang XK (2009) Adsorption of Eu(III) onto TiO_2: effect of pH, concentration, ionic strength and soil fulvic acid. J Hazard Mater 168:458–465

Vargas R, Madriz L, Márquez V, Torres D, Kadirova ZC, Yubuta K, Hojamberdiev M (2022) Elucidating the enhanced photoelectrochemical performance of zinc-blende ZnS/wurtzite ZnO heterojunction and adsorption of water molecules by molecular dynamics simulations. Mater Sci Semicond Process 142:106494

Wang DJ, Jin Y, Jaisi DP (2015) Cotransport of hydroxyapatite nanoparticles and hematite colloids in saturated porous media: Mechanistic insights from mathematical modeling and phosphate oxygen isotope fractionation. J Contam Hydrol 182:194–209

Wang KK, Ma Y, Sun BB, Yang Y, Zhang YQ, Zhu LY (2022) Transport of silver nanoparticles coated with polyvinylpyrrolidone of various molecular sizes in porous media: Interplay of polymeric coatings and chemically heterogeneous surfaces. J Hazard Mater 429:128247

Wei XY, Sun YL, Pan DQ, Niu Z, Xu ZW, Jiang YJ, Wu WS, Li ZB, Zhang L, Fan QH (2019) Adsorption properties of Na-palygorskite for Cs sequestration: effect of pH, ionic strength, humic acid and temperature. Appl Clay Sci 183:105363

Xi XL, Wang L, Zhou T, Yin J, Sun HM, Yin XQ, Wang N (2022) Effects of physicochemical factors on the transport of aged polystyrene nanoparticles in saturated porous media. Chemosphere 289:133239

Xu WP, Liu CS, Zhu JM, Bu HL, Tong H, Chen MJ, Tan DC, Gao T, Liu YZ (2022) Adsorption of cadmium on clay-organic associations in different pH solutions: the effect of amphoteric organic matter. Ecotoxicol Environ Saf 236:113509

Yadav BS, Dasgupta S (2022) Effect of time, pH, and temperature on kinetics for adsorption of methyl orange dye into the modified nitrate intercalated MgAl LDH adsorbent. Inorg Chem Commun 137:109203

Yang QQ, Li ZY, Lu XN, Duan QN, Huang L, Bi J (2018) A review of soil heavy metal pollution from industrial and agricultural regions in China: pollution and risk assessment. Sci Total Environ 642:690–700

Ying SX, Guan ZR, Ofoegbu PC, Clubb P, Rico C, He F, Hong J (2022) Green synthesis of nanoparticles: Current developments and limitations. Environ Technol Innov 26:102336

Zhang YH, Liao M, Guo JW, Na Xu, Xie XM, Fan QY (2022) The co-transport of Cd(II) with nanoscale As_2S_3 in soil-packed column: effects of ionic strength. Chemosphere 286:131268

Zhao Y, Shao ZY, Chen CL, Hu J, Chen HL (2014) Effect of environmental conditions on the adsorption behavior of Sr(II) by Na-rectorite. Appl Clay Sci 87:1–6

Zhao TH, Fang MY, Tang Z, Giesy JP (2019) Adsorption, aggregation and sedimentation of titanium dioxide nanoparticles and nanotubes in the presence of different sources of humic acids. Sci Total Environ 692:660–668

Zhao J, Li Y, Wang XJ, Xia X, Shang EX, Ali J (2021) Ionic-strength-dependent effect of suspended sediment on the aggregation, dissolution and settling of silver nanoparticles. Environ Pollut 279:116926

Zheng ZY, Zhu S, Lv MM, Gu ZJ, Hu HX (2022) Harnessing nanotechnology for cardiovascular disease applications—a comprehensive review based on bibliometric analysis. Nano Today 44:101453

Zhou DX, Keller AA (2010) Role of morphology in the aggregation kinetics of ZnO nanoparticles. Water Res 44:2948–2956